GEODYNAMICS & TECTONOPHYSICS

PUBLISHED BY THE INSTITUTE OF THE EARTH'S CRUST
SIBERIAN BRANCH OF RUSSIAN ACADEMY OF SCIENCES

2015 VOLUME 6 ISSUE 1 PAGES 77–89 ISSN 2078-502X

http://dx.doi.org/10.5800/GT-2015-6-1-0173

STRUCTURE OF THE LITHOSPHERE AND SEISMOTECTONIC DEFORMATIONS IN CONTACT ZONE OF LITHOSPHERIC PLATES IN THE SUMATRA ISLAND REGION

O. A. Kuchay[1], N. A. Bushenkova[1, 2], A. A. Tataurova[2]

[1] *Trofimuk Institute of Petroleum Geology and Geophysics, Siberian Branch of RAS, Novosibirsk, Russia*
[2] *Novosibirsk State University, Novosibirsk, Russia*

Abstract: The inversion seismic tomography algorithm (ITS) was used to calculate 3D seismic anomalies models for velocities of P- and S-waves in the zone of the Sunda arc, Indonesia. In the area under study, strong earthquakes (M>4.8) are clustered in the zone of high P-wave velocities. Earthquake hypocenters are located in zones of both high and low velocity anomalies of S-waves. The giant Sumatra earthquake (December 26, 2004, Mw=9.0) ruptured the greatest fault length of any recorded earthquake, and the rupture started in the area wherein the sign of P-wave velocity anomalies is abruptly changed. We calculated seismotectonic deformations (STD) from data on mechanisms of 2227 earthquakes recorded from 1977 to 2013, and our calculations show that the STD component, that controls vertical extension of rocks, is most stable through all the depth levels. In the marginal regions at the western and eastern sides of the Sunda arc, the crustal areas (depths from 0 to 35 km) are subject to deformations which sign is opposite to that of deformations in the central part. Besides, at depths from 70 to 150 km beneath the Sumatra earthquake epicentre area, the zone is subject to deformations which sign is opposite to that of deformations in the studied part of the Sunda arc. For earthquakes that may occur in the crust in the Sunda arc in the contact zone of the plates, maximum magnitudes depend on the direction of pressure imposed by the actively subducting plate, which is an additional criteria for determining the limit magnitude for the region under study.

Key words: anomalies of P- and S-wave velocities, the Sunda arc, seismotectonic deformations, limit magnitude.

Recommended by Yu.L. Rebetsky

For citation: *Kuchay O.A., Bushenkova N.A., Tataurova A.A.* 2015. Structure of the lithosphere and seismotectonic deformations in contact zone of lithospheric plates in the Sumatra Island region. *Geodynamics & Tectonophysics* 6 (1), 77–89. doi:10.5800/GT-2015-6-1-0173.

СТРУКТУРА ЛИТОСФЕРЫ И СЕЙСМОТЕКТОНИЧЕСКИЕ ДЕФОРМАЦИИ ЗОНЫ КОНТАКТА ЛИТОСФЕРНЫХ ПЛИТ В РАЙОНЕ ОСТРОВА СУМАТРА

О. А. Кучай[1], Н. А. Бушенкова[1, 2], А. А. Татаурова[2]

[1] *Институт нефтегазовой геологии и геофизики им. А.А. Трофимука СО РАН, Новосибирск, Россия*
[2] *Новосибирский государственный университет, Новосибирск, Россия*

Аннотация: На основе сейсмотомографического алгоритма ИТС рассчитано трехмерное распределение аномалий скоростей P- и S-волн в зоне Зондской дуги. Сильные землетрясения (с M>4.8) рассматриваемого райо-

на группируются в зоне повышенных скоростей P-волн. Гипоцентры сейсмических событий попадают в зоны как повышенных, так и пониженных скоростей S-волн. Географически начало вспарывания очага Суматранского землетрясения 2004 г. (Mw=9.0) совпадает с районом резкого изменения знака аномалий скоростей P-волн. Расчет сейсмотектонических деформаций по данным механизмов 2227 землетрясений, зарегистрированных с 1977 по 2013 г., показал, что на всех глубинах наиболее устойчиво ведет себя компонента СТД, отвечающая за вертикальное удлинение объемов горных масс. Участки земной коры (0–35 км) в окраинных районах с западной и восточной стороны Зондской дуги характеризуются деформациями противоположного знака по отношению к центральной части. Также в слое 70–150 км под эпицентральной областью Суматранского землетрясения происходят деформации противоположного знака по отношению к деформациям рассматриваемой части Зондской дуги. Максимальные магнитуды коровых землетрясений Зондской дуги, возникающие в зоне контакта плит, зависят от направления давления активной погружающейся плиты, что является одним из дополнительных критериев определения предельной магнитуды этого района.

Ключевые слова: аномалии скоростей P- и S-волн, Зондская дуга, сейсмотектонические деформации, предельная магнитуда.

1. Introduction

The giant Sumatra earthquake (December 26, 2004, Mw=9.0) has become a subject of many interesting publications both abroad [*Cheng Zong-yi, Zhu Wen-yao, 2001; Chlieh et al., 2007; Dewey et al., 2007; Engdahl et al., 2007; Vallee, 2007*] and in Russia [*Rebetskii, Marinin, 2006; Shevchenko et al., 2006*]. With account of the fact that it was followed by several strong seismic events near the Sumatra Island, our idea was to conduct a detailed study of seismotectonic deformations (STD) and recent earthquakes. We reviewed data on earthquake focal mechanisms (M>4.8) in the Sunda subduction zone [*The Global Centroid-Moment-Tensor..., 2015*] and estimated STD values for the following depths: 0–35 km (1450 solutions of earthquake focal mechanisms), 36–70 km (539 solutions), 71–105 km (156 solutions), 106–150 km (43 solutions), and 151–300 km (29 solutions). Thicknesses of the layers were determined with account of the availability of data on earthquake foci mechanisms. We checked several options for determining a thickness of a layer for which we estimated STD with application of models showing anomalies of P- and S-wave velocities at various depths. In many cases, we were not satisfied with a number of seismic event records in the given layer, and thus decided to focus our attention on the option with the solutions specified above.

The Sunda arc represents a convergent margin and reflects processes of interaction between the Indo-Australian and Eurasian lithospheric plates that are approaching each other. This movement takes place along the Andaman, Nicobar, Sumatra and Java islands. Seismicity is high in the subduction zone. It should be noted that the density of earthquake hypocentres with M>4.8 decreases with depth, and only a few strong seismic events were recorded at depths below 200 km. Hypocentres of seismic events migrate from the deep-water trough towards the Sumatra and Java islands. The deepest seismic events took place underneath the Barisan ridge with recent volcanism. Earthquakes of thrust (60 %), shear (15 %) and normal-fault (25 %) types occurred in the crust to depths of 70 km. At depths from 70 to 250 km, cases of shearing are rare, and 75–80 % foci were associated with thrusting, and 15–20 % foci with normal faulting.

In the focal area of the giant Sumatra earthquake of December 2004, thrusting took place along the gently sloping plane in the west–south-western direction [*The Global Centroid-Moment-Tensor..., 2015*]. In the horizontal plane, the focal area is 1000 km long. Similar focal mechanisms are typical of the strongest aftershocks and earthquakes recorded both before and after the Sumatra earthquake, except seismic events of the shear type near Andaman and Nicobar islands. The pattern of the majority of fault planes of the seismic events correlates with the strike of the Sunda arc.

It is logical to suggest that deep processes and the structure of the crust and the lithospheric mantle play an important role in the distribution of deformation and the occurrence of the earthquake foci.

2. Tomography modelling method

The velocity structure of the Sumatra Island region has been studied for many years, yet remains insufficiently investigated for constructing a comprehensive geodynamic model that would unambiguously show the development of the territory under study. Seismic

tomography technologies are now widely applied in studies of velocity patterns at depths. The available models either represent separate local reconstructions or show results of global studies with low resolution levels due to insufficient quantities or quality of analysed data, such as global models of mantle inhomogeneities [*Hafkenscheid et al., 2001; Van der Hilst et al., 1997*], local crust models to the 10 km depth for the Krakatau region [*Jaxybulatov et al., 2011*] and others.

We studied the seismic pattern of the mantle by applying the inversion tomographic scheme (ITS). Initially, ITS was proposed as an alternative to the traditional direct teleseismic scheme applied to studying high seismicity regions wherein the seismic networks failed to provide for tomographic inversion of proper quality [*Koulakov*, *1998*]. The main prerequisite for using ITS is the availability of records by stations of the global seismic networks of a sufficient number of seismic events in the study area. In the earlier versions of ITS [*Koulakov et al., 2002; Kulakov et al., 2003*], only teleseismic rays were applied, and sources were not relocated. In the next version of ITS [*Koulakov et al*., *2006*], which is applied in our study, all possible rays available in the catalogues are used. Rays with small epicentral distances provide for preliminary determinations of sources' locations, and rays with large epicentral distances are used to determine the regional deep seismic structure. The ITS algorithm uses the arrival time of seismic P- and S-waves from earthquakes inside the studied region, which were recorded by stations of the global seismic network. Based on the algorithm, it is possible to calculate 3D patterns of anomalies of P- and S-wave velocities and locations of seismic sources.

In our study, the tomographic inversion was calculated in three circular windows with specified coordinates and radius, which are overlapping each other. The circle radius is close by value to the depth of the area under study. To study the upper mantle, the radius is accepted at ~1000 km. For each circular window, we selected data on seismic sources located inside such circles, and inversion was carried out with two parametrization grids of different orientations. Inversion results for the circular windows were consolidated into one model. The ITS algorithm is based on the linearized approach envisaging calculation of seismic anomalies during one iteration of inversion on the basis of rays in a one-dimensional model since for obtaining stable results, it is required to process huge volumes of data from the International Seismological Centre (ISC) catalogue (with a high noise factor). Applying non-linear approaches (mainly, 3D ray tracing) makes the task more cumbersome. Moreover, relatively small variations of seismic velocities in the upper mantle (maximum 5 %) do not cause any significant changes in the path of the rays and, correspondingly, do not lead to calculating errors. In our study, we used the algorithm that is described in detail in [*Koulakov et al., 2006*].

For our study, we took data on seismic events from the ISC catalogue for the period from 1964 to 2007, and used the arrival times recorded by stations of the global seismic network (10000+). Within the entire study region, we selected 2110 seismic events which travel times are known (more than 200000 times for P- and over 180000 times for the S-rays). Inversion was carried out in the three overlapping circular windows, each with a radius of 8°. Locations of all the earthquakes, which data were taken from the ISC catalogue, were recalculated under the options of the above-mentioned algorithm, and outlying values were screened out and rejected (more than 15 % in the ISC catalogue).

Upon inversion in the circular windows, the root-mean-square (RMS) time residual for the used data was reduced by 35 to 45 %, depending on the circle. Relatively small reduction of the time residual is due to a high noise factor in the data and the low-contrast structure of inhomogeneities in the upper mantle. Results of inversion of the real data for anomalies of P- and S-wave velocities are shown in horizontal sections (see Fig. 1, *a*, *b*, *c*, *d*, *e*). A correlation between patterns of anomalies of P- and S-wave velocities is evident, which is an indirect confirmation that the proposed models are reliable. Across the region, the anomalies are most contrasting to a depth of 200 km (amplitudes of ~3.5 %); at the lower depths of the mantle, they become less contrasting. It should be borne in mind that tomographic inversion generally yields lower amplitudes of anomalies, which is shown in [*Koulakov et al*., *2006*] by results of synthetic testing of the algorithm. Uncertainty with amplitude anomalies reconstruction is a common problem of tomography, which arises in any similar study. In our assumption for the given case, the real amplitude of the anomalies may average higher by a factor of 1.5–2.0 than the obtained results. The tomographic model of the Sumatra-Andaman zone shows anomalies with higher P-wave velocities at different depths (50 km, 100 km, 150 km, and 220 km; see Fig. 1, *a*, *b*, *c*, *d*, *e*). When using the regional seismic tomography schemes, as in our case, it is technically impossible to determine the detailed structure of the upper 50-km layer (i.e. the crust) because the path of teleseismic rays at such depths is practically vertical. When applying the seismic tomography method to study the structure of the crust, it is required to have a large database of uniformly distributed local seismic data, to which it would be possible to apply local seismic tomography schemes. In the given case, we did not have the materials from the local network. Therefore, the results obtained for the depth of 50 km were used twice, when seismotectonic

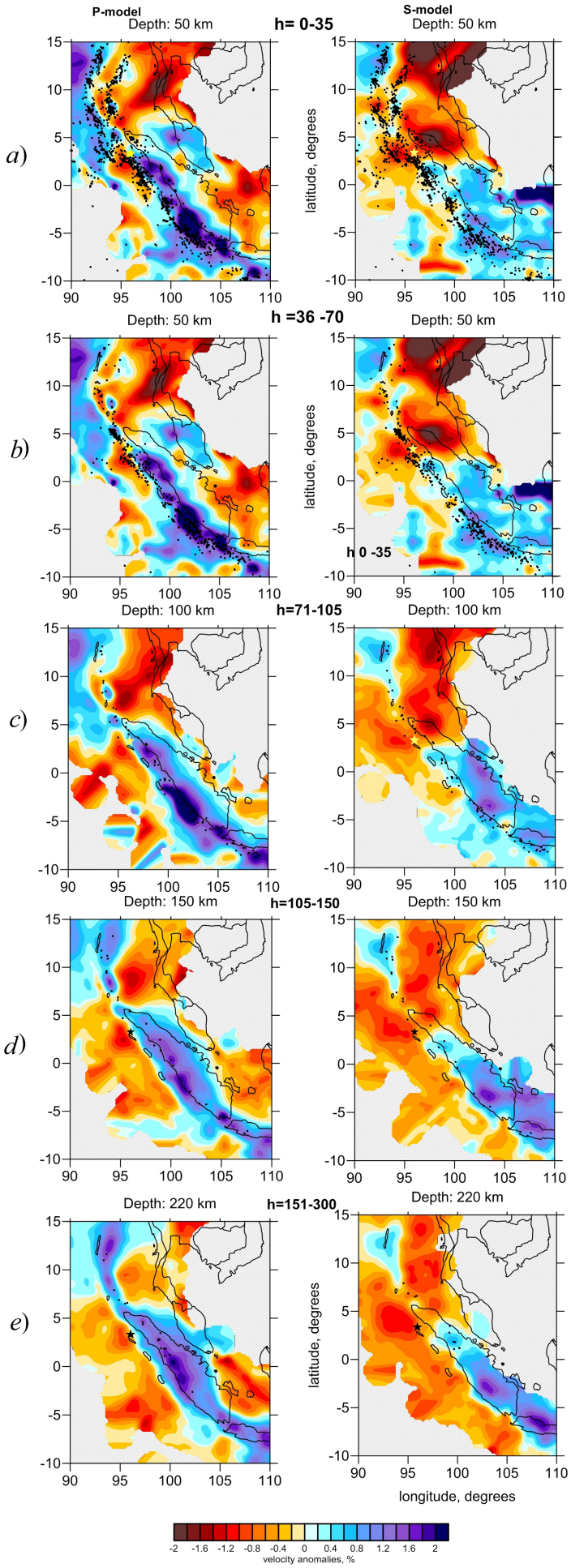

Fig. 1, *a*, *b*, *c*, *d*, *e* – anomalies of seismic P- and S-wave velocities at depths of 50, 100, 150, and 220 km.

Areas of high P- and S-wave velocities are shaded in blue; areas of low P- and S-wave velocities are shaded in red-brown. Velocity anomalies are given in percentage values in the column at the bottom of the figure. Epicentres close to the corresponding depths are shown by black and red circles. Yellow and black asterisks show start locations of the rupture in the 2004 Sumatra earthquake focal area.

Рис. 1, *a*, *b*, *c*, *d*, *e*. – аномалии скоростей сейсмических P- и S-волн на глубинах 50, 100, 150, 220 км.

Синие тона – зоны с повышенными значениями скоростей P- и S-волн; красно-коричневые тона – зоны пониженных скоростей P- и S-волн. Внизу рисунка показана колонка градаций аномалий скоростей в процентном отношении. Черным и красным отмечены эпицентры землетрясений, близких к соответствующим глубинам срезов. В виде звезд желтого или черного цвета отмечены местоположения начальной точки вспарывания в очаге Суматранского землетрясения 2004 г.

deformations were compared in the layer 0–35 km and in the layer 36–70 km.

3. Analysis of tomographic model calculations and distribution of earthquake foci

By analyzing of the distribution of earthquake epicentres in the maps of increasing and decreasing velocity of compressional and shear waves, we found that the majority of seismic events (M> 4.8) in the study region are clustered within the zone of high velocity of P-waves (see Fig. 1, *a*, *b*, *c*, *d*, *e*). It is most obvious for earthquakes at depths from 36 to 70 km (for the depth of 50 km, the velocity field is reconstructed). Deeper earthquake sources (70–300 km) are concentrated only in areas of high velocity of P-waves (see Fig. 1, *c*, *d*, *e*). Hypocentres of seismic events are revealed in zones of both high and low velocity of S-waves (Fig. 1, *a*, *b*, *c*, *d*, *e*). An interesting fact is that the rupture associated with the Sumatra earthquake (December 26, 2004, Mw=9.0) started in the area characterized by an abrupt change of the sign of P-wave velocity anomalies (see Fig. 1, *a*).

4. Seismotectonic deformation calculation method

The western part of the Sunda arc has been the subject of many studies aimed at analyses of parameters of earthquake foci mechanisms. A reconstruction of the stress field before the giant Sumatra earthquake of 2004 was published in [*Rebetskii, Marinin*, *2006*] that we believe to be the most interesting work. There were attempts to reconstruct the field of stresses and strain in different areas of this territory [*Kundu, Gahalaut*, *2011; Radha Krishna, Sanu, 2002; Shevchenko et al., 2006*]. However, detailed analysis of seismotectonic deformations at different depth layers has not been executed yet. Therefore, we propose using the method published in [*Riznichenko*, *1985*; *Kostrov*, *1975*] to estimate deformations of rock masses which took place at different depths due to earthquake, as follows: the tensor of seismotectonic deformations equals the sum of seismic moment tensors of all the earthquakes that occurred in the unit volume within a specified period of time:

$$\mathrm{E}_{lm} = \frac{1}{\mu V T} \sum_{n=1}^{N} M_0^{(n)} Q_{lm}^{(n)},$$

where μ – shear modulus; V – averaging volume; $M_0^{(n)}$ – seismic moment of n-th earthquake; $Q_{lm}^{(n)}$ – components of the directional unit tensor of seismic moment of n-th earthquake in the geographic coordinate expressed in the foci mechanism parameters. The value $M_0^{(n)}$ is a weight factor calculated from the earthquake energy class/magnitude. Deformation of areas, wherein medium and strong earthquakes took place, is mainly determined by strong seismic events. Calculations through the entire region vary in the level of detail as some of the smoothing windows contain only one or two earthquakes. Within each elementary averaging window, we calculate components of the tensor of incremental seismotectonic deformations (STD). In our case, division by time (T) is not carried out, and the total seismotectonic deformation is calculated for the entire period of observations at different depth levels.

For the tectonic plate contact area, seismotectonic deformations are calculated from data on mechanisms of 2227 earthquakes recorded from 1977 to 2013 [*The Global Centroid-Moment-Tensor..., 2015*]. Taking into account their uneven distribution within the region under study, we select an averaging area that is large enough (1°×1°; 0.5° spacing). The averaging area for the strongest events are twice as large. For the purposes of mapping, important are not values of deformation, but their signs, i.e. relative elongation / shortening of deformations due to the earthquakes. In this paper, positive/negative values of deformations correspond to relative elongation/shortening of linear dimensions of elementary volumes of the crust in the corresponding directions.

5. Analysis of calculated fields of latitudinal, meridional and vertical components of seismotectonic deformations (STD)

In the field of the latitudinal component of STD, the crustal layer (0–35 km) is mainly subject to shortening deformation (negative values), while elongation deformation (positive values) are revealed in the marginal parts of the submeridional zone and in the northern part (Fig. 2, *a*). The field of the meridional component of STD is more uniform and characterized mainly by negative values. Small areas of positive values are located in the marginal zones, i.e. in the northern (near the Andaman and Nicobar Islands) and southern parts of the study region (see Fig. 2, *a*). Positive values are a specific feature of the vertical component of deformations. Areas with negative values are located outside the fault bordering the Sunda arc from the west and south-west, as well as at the eastern side of the Sumatra fault (see Fig. 2, *a*). Of the three components, the highest values are typical of the vertical component of STD.

In the next layer (36–70 km), the deformation pattern is simpler, and values of the latitudinal and meridional components are predominantly negative, and positive in the northern part. The field of the vertical

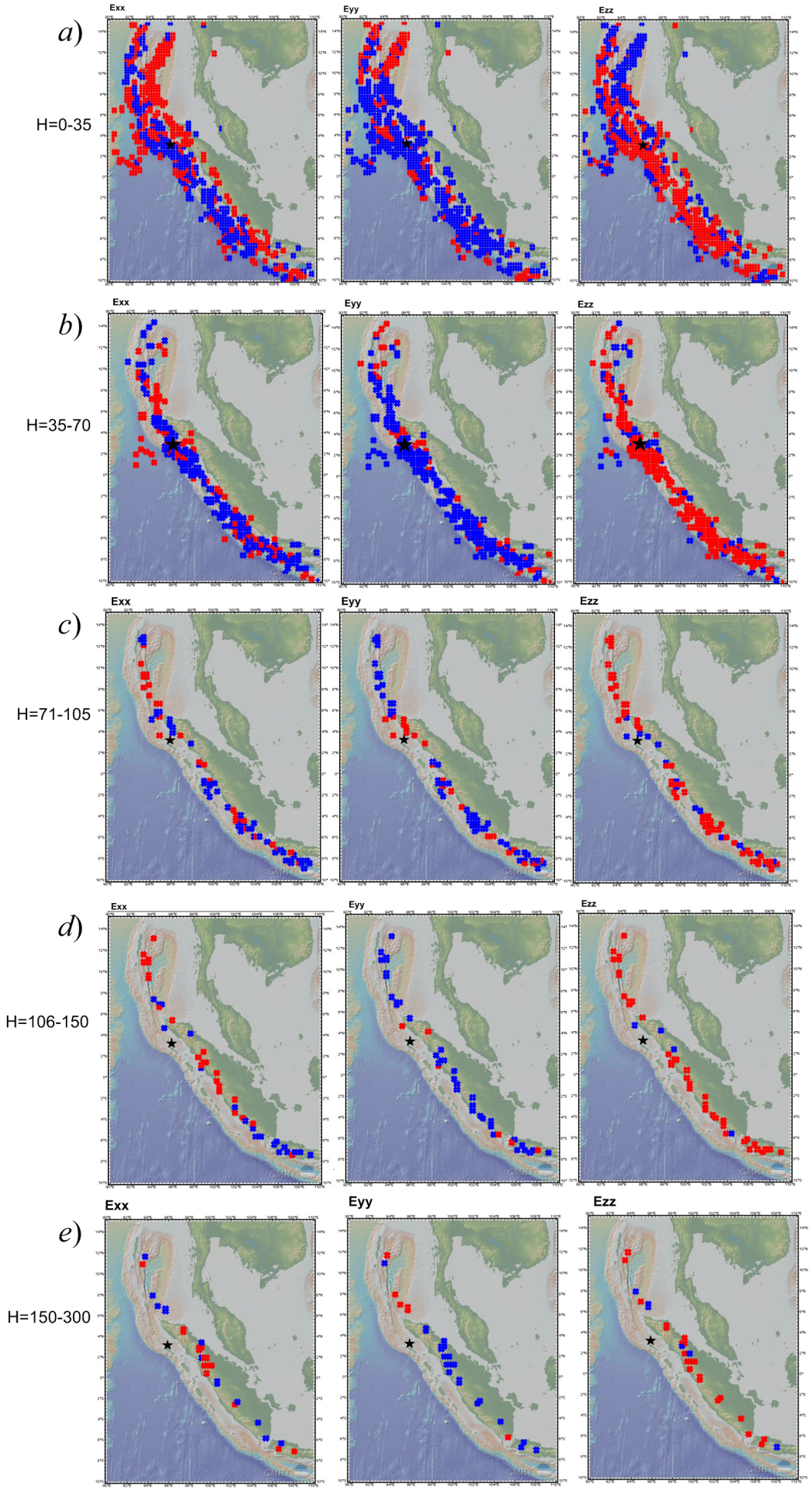
a)
H=0-35
Exx
Eyy
Ezz
b)
H=35-70
Exx
Eyy
Ezz
c)
H=71-105
Exx
Eyy
Ezz
d)
H=106-150
Exx
Eyy
Ezz
e)
H=150-300
Exx
Eyy
Ezz

Fig. 2. Latitudinal (Exx), meridional (Eyy) and vertical (Ezz) components of seismotectonic deformations according to calculations from focal mechanisms of earthquakes (M>4.8) from 1976 to 2013: (*a*) H=0–35 km, (*b*) H=36–70 km, (*c*) H=71–105 km, (*d*) H=106–150 km, (*e*) H=150–300 km.

Columns showing data on components: left – latitudinal, central – meridional, right – vertical. Colour codes of areas marked by boxes: shortening – blue, extension – red. The 2004 Sumatra earthquake epicentre is shown by the asterisk.

Рис. 2. Широтная (Exx), меридиональная (Eyy) и вертикальная (Ezz) компоненты сейсмотектонических деформаций, рассчитанные по данным механизмов очагов землетрясений, произошедших в период с 1976 по 2013 г. с M>4.8: (*a*) H=0–35 км, (*b*) H=36–70 км, (*c*) H=71–105 км, (*d*) H=106–150 км, (*e*) H=150–300 км.

Колонка слева – поле широтной компоненты, колонка в центре – поле меридиональной компоненты, колонка справа – поле вертикальной компоненты. Синими цветами отмечены укорочения, красными – удлинения объемов горных масс в соответствующих направлениях. Эпицентр Суматранского землетрясения отмечен звездочкой.

component also maintains the mode of deformation of the upper part of the crust (Fig. 2, *b*).

In the subducting plate, at depths of 70–105 km and 106–150 km, volumes of rock masses are subject mainly to vertical extension and meridional shortening. Meridional elongation and vertical shortening are observed beneath the central part of the epicentral area of the Sumatra earthquake (Fig. 2, *c*, *d*). In the latitudinal component (Exx) of deformation, for the upper and lower layers (71–105 km and 106–150 km, respectively), positive values are revealed in the area of the Andaman and Nicobar Islands. Southward, the deformation field (at depths from 71 to 105 km) is lacking uniformity and contains alternating areas of extension and shortening (see Fig. 2, *c*, *d*). At depths from 106 to 150 km, positive values of the latitudinal component of deformation are revealed to the south of the epicentral area of the 2004 earthquake, and negative values are noted in the southern part of the sublatitudinal area (Fig. 2, *d*). At depths from 150 to 300 km, the number of earthquakes is minimum, and it is possible only with reserve to talk about meridional shortening and latitudinal and vertical extension of rock masses in the central part of the study region. But the vertical component has positive values through virtually the entire region covered by our analyses (Fig. 2, *e*). Generally, the meridional component of deformation has negative values in all depth ranges, with the exception of the source area of the Sumatra earthquake wherein rock masses at depth from 71 to 150 km are subject to meridional shortening (see Fig. 2, *c*). Reviewing seismotectonic deformations in the thinner layer, 71–130 km, reveals similar specific features of the deformation pattern in the central part of the source area (Fig. 3).

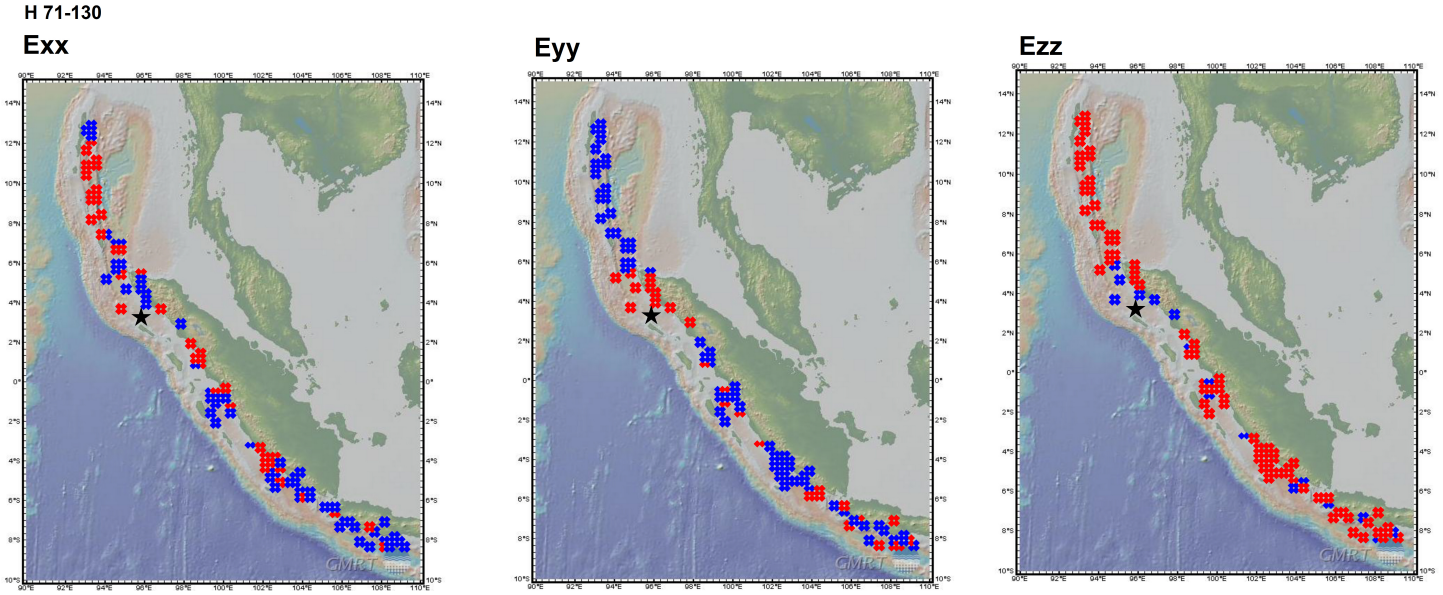

Fig. 3. Latitudinal (Exx), meridional (Eyy) and vertical (Ezz) components of seismotectonic deformations according to calculations from focal mechanisms of earthquakes at depths from 71 to 130 km.

Рис. 3. Широтная (Exx), меридиональная (Eyy) и вертикальная (Ezz) компоненты сейсмотектонических деформаций по данным механизмов очагов землетрясений, зарегистрированных в диапазоне глубин H=71–130 км.

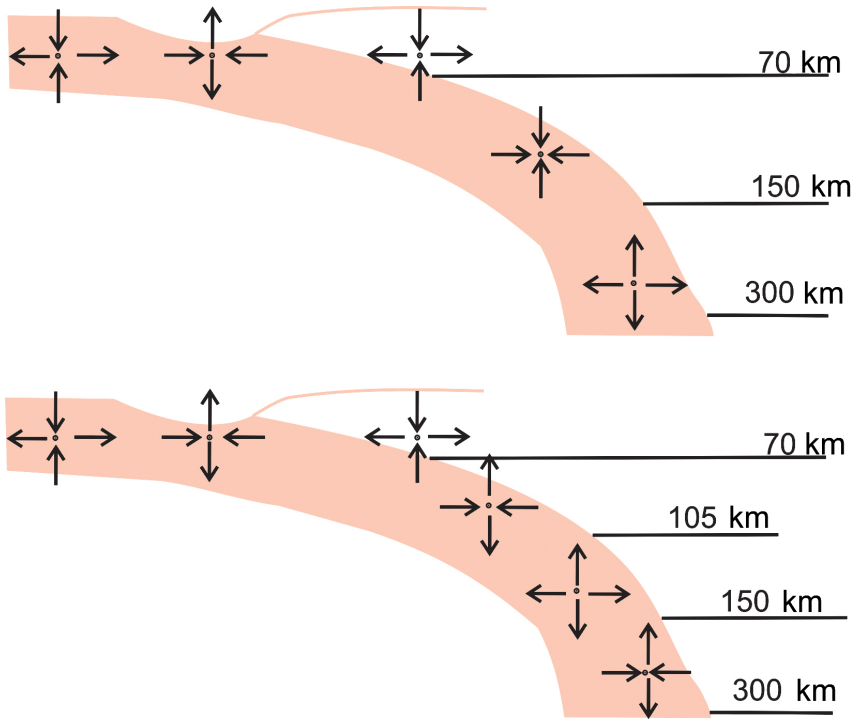

Fig. 4. The pattern of extension and shortening areas in the vertical plane along the parallel across the hypocentral area of the Sumatra earthquake in the contact zone of the Indo-Australian and Eurasian plates (top scheme) and along the parallel at 4°S latitude. The subducting plate is shaded in pink.

Рис. 4. Схема распределения удлинений и укорочений в вертикальной плоскости вдоль параллели через гипоцентральную область Суматранского землетрясения в зоне контакта Индо-Австралийской и Евроазиатской плит (верхняя схема) и вдоль параллели через 4 градус ю.ш. Розоватым тоном показана погружающаяся плита.

Based on analyses of the obtained results, two sections are constructed, one along the parallel across Sumatra earthquake hypocentre, and another southward of the equator at 4° S latitude. According to Figure 4, at all depths, the most stable behaviour is demonstrated by the vertical extension component of STD, and, to some extent, by the meridional shortening component. The STD analysis shows that at depths from 71 to 150 km beneath the Sumatra earthquake epicentre area, deformation takes place with an opposite sign with respect to deformations of the Sunda arc (Fig. 4).

No dependence has been revealed by attempts to correlate the areas of extension and shortening of the field of the latitudinal, meridional and vertical components of STD with specific features of changes in velocities of compressional and shear waves, as evidenced by the below figures for a range of depths (Fig. 5).

6. The displacement direction of the Indo-Australian plate and the distribution of strong earthquakes

We used data on strong earthquakes' epicentres in the western part of the Sunda subduction arc (the contact zone of the Indo-Australian and Eurasian plates) to investigate the amount of energy of a strongest earthquake that may occur in the contact zone of these plates, depending on the angle between the horizontal displacement of the Indo-Australian plate and the stretch of the contact area. In the studied segment of the Indo-Australian plate, the amount of displacement is practically unchanged. In our assumption, a seismic event is within the zone impacted by the contact between the two plates, if its focus is away from the contact zone by no more than 100 km. This width of the zone is determined by both positional accuracy and dimensions of strong earthquakes' foci.

For our analyses, the contract zone of the two plates was divided into intervals wherein the zone's stretch has not changed (Fig. 6). We measured the angles between the stretch of the contact (zone) and the displacement direction of the Indo-Australian Plate. Since seismic events with M=6 occurred in the crust across the entire selected region, all the registered earthquakes with M≥7 (from 1977 to 2013) are plotted (Fig. 7) with magnitudes shown as a function of angles between the displacement direction of the plate [*Chlieh et al., 2007*] and the line of contact plates. Data from [*Chlieh et al., 2007*] on the strongest earthquakes of the

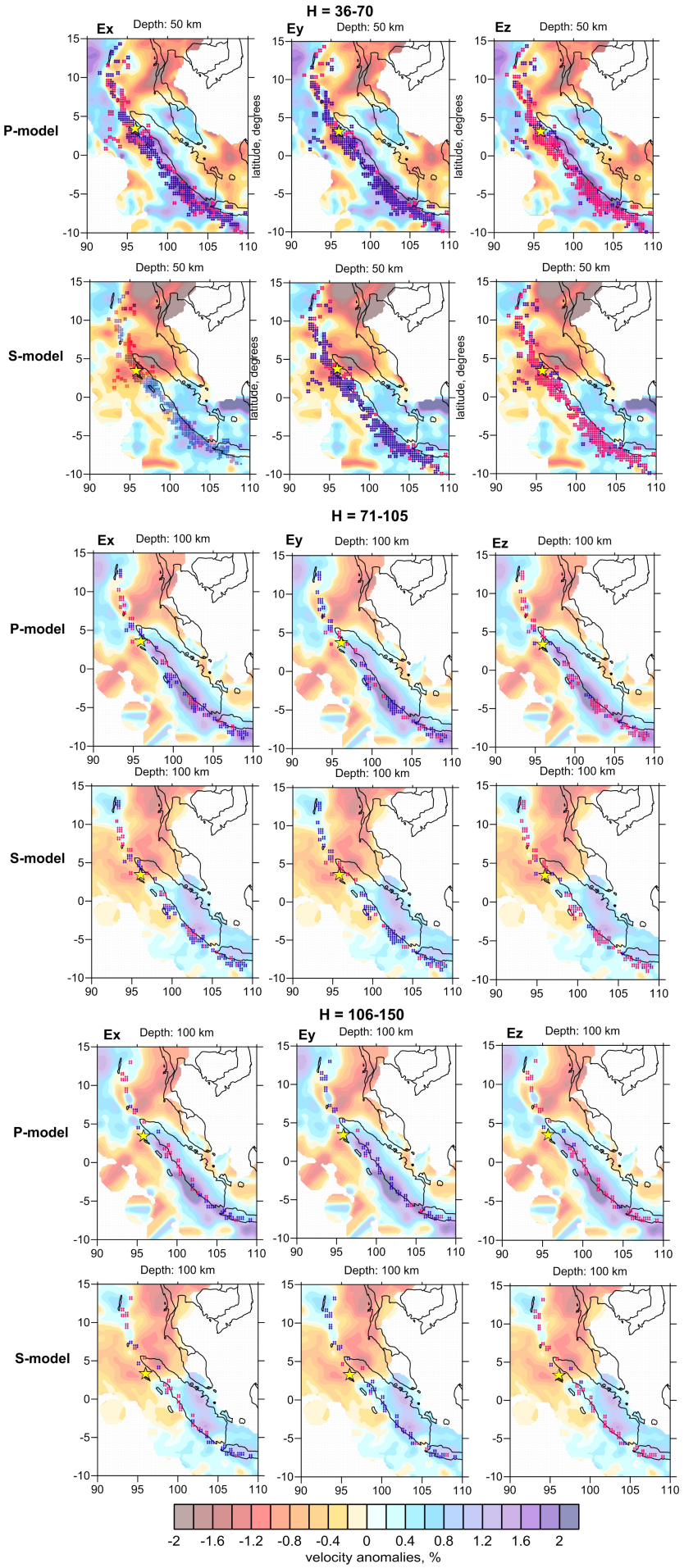

Fig. 5. Latitudinal, meridional and vertical components of seismotectonic deformations according to calculations from earthquake focal mechanisms (M>4.8) at the background of anomalies of seismic P- and S-wave velocities at depths of 50, 100, and 150 km.

Colour codes of areas marked by boxes: shortening – dark blue; extension – red. Areas with high values of P- and S-wave velocities are shaded in blue, low-velocity areas – in orange-brown. The 2004 Sumatra earthquake epicentre is shown by the asterisk. Velocity anomalies are given in percentage values in the column at the bottom of the figure.

Рис. 5. Широтная, меридиональная и вертикальная компоненты сейсмотектонических деформаций, полученных по данным механизмов очагов землетрясений с M>4.8, на фоне аномалий скоростей сейсмических P- и S-волн на глубинах 50, 100, 150 км.

Темно-синими квадратами показаны области укорочения, красными – удлинения. Синие тона – зоны с повышенными значениями скоростей P- и S-волн, оранжево-коричневые тона – зоны пониженных скоростей. Эпицентр Суматранского землетрясения отмечен звездочкой. Внизу показана колонка градаций аномалий скоростей в процентном отношении.

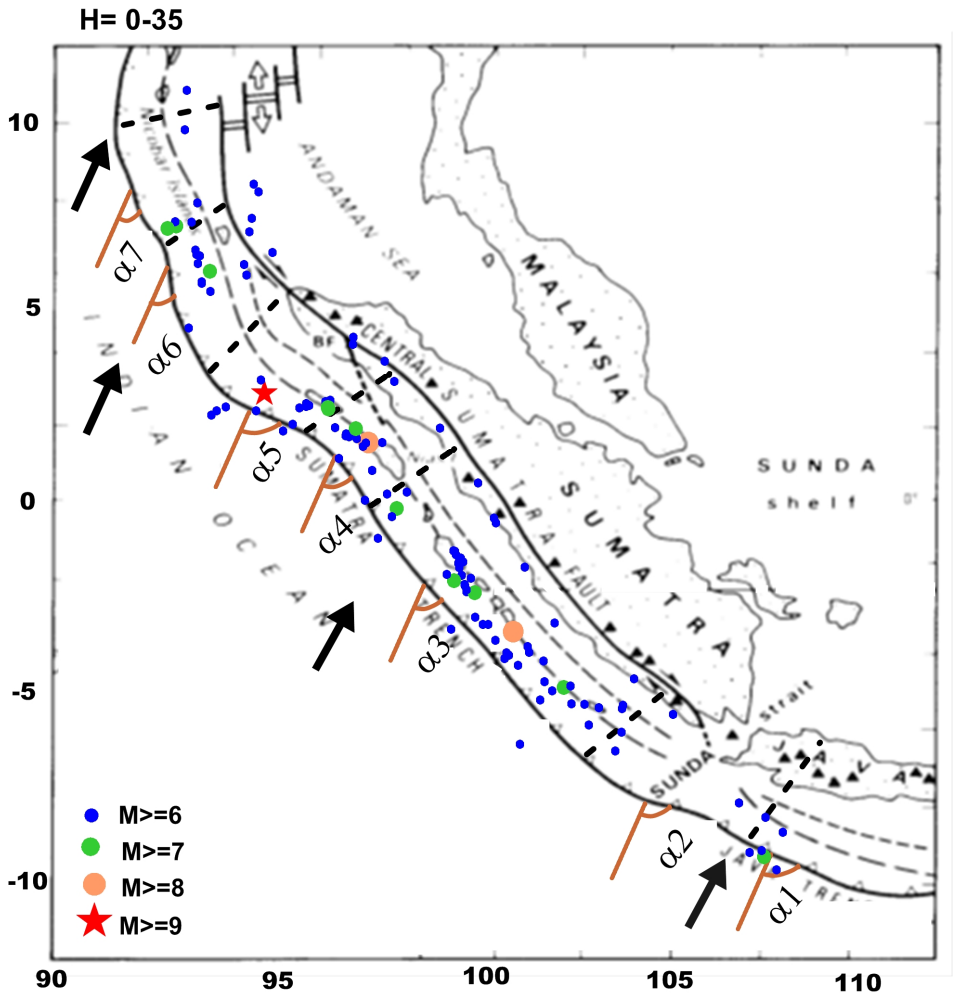

Fig. 6. Locations of earthquake epicentres (Ms≥7) in the contact zone of the Indo-Australian and Eurasian plates.

The contact zone's scheme is taken from [*Huchon, Le Pichon, 1984*]. α1, α2, α3 etc. (brown) – angles between the displacement direction of the Indo-Australian lithospheric plate and the stretch of contact zone of the two plates. Black dashed lines separate areas within which the stretch is maintained. Arrows show the displacement direction of the Indo-Australian plate, according to [*Chlieh et al., 2007*]. Earthquake epicentres are shown according to [*The Global Centroid-Moment-Tensor…, 2015*].

Рис. 6. Расположение эпицентров землетрясений с Ms>=7 в зоне контакта Индо-Австралийской и Евроазиатской плит.

Схема зоны контакта использована из статьи [*Huchon, Le Pichon, 1984*]. Коричневым цветом показаны углы между направлением смещения Индо-Австралийской литосферной плиты и зоной контакта двух плит. Эти углы обозначены как α1, α2, α3 и т.д. Черными штриховыми линиями отделены участки, в пределах которых простирание практически не меняется. Стрелками показано направление смещения Индо-Австралийской плиты [*Chlieh et al., 2007*]. Эпицентры землетрясений нанесены по данным [*The Global Centroid-Moment-Tensor…, 2015*].

past years are also used. The most powerful earthquakes occurred in segments of the zone wherein the angles are close to 80 degrees. In Figure 7, the limiting contour shows a possible maximum magnitude of a seismic event that may occur in different parts of the Sunda arc. Thus, for earthquakes that may occur in the crust in the contact zone of the plates, maximum magnitudes depend on the direction of pressure imposed by the actively subducting plate, which is an additional criterion for determining the limit magnitude for the study region.

7. Conclusion

In the Sumatra Island region, the strong earthquakes (M>4.8) are clustered in the zone of high P-wave velocities. The hypocentres of the seismic events are revealed in the zones of both high and low velocities of S-waves.

Ripping at the source of the Sumatra earthquake (December 26, 2004, Mw=9.0) started in the area characterized by an abrupt change of the sign of P-wave velocity anomalies.

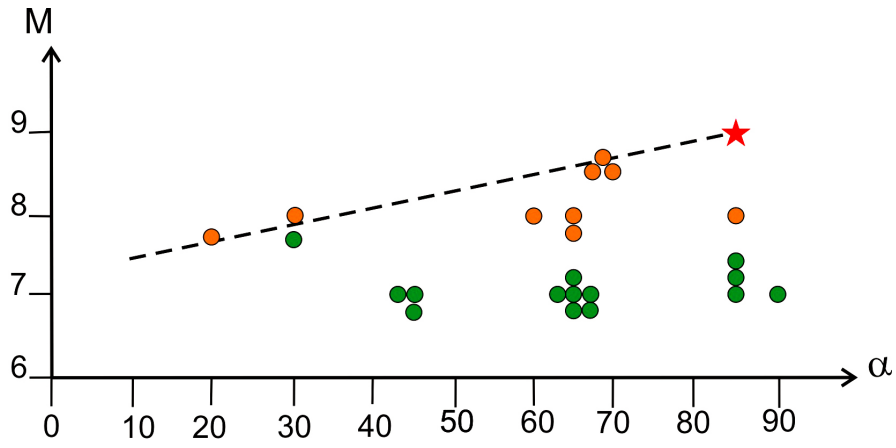

Fig. 7. The dependence of the limit magnitude of earthquake in the contact zone of the Indo-Australian and Eurasian plates on the angle between the displacement direction of the Indo-Australian lithospheric plate and the stretch of contact zone.

The plot is based on historical earthquake data from [*Chlieh et al., 2007*]. Color codes are the same as in Fig. 6.

Рис. 7. Зависимость предельной магнитуды землетрясений, возникших в зоне контакта Индо-Австралийской и Евроазиатской плит, от угла между направлением смещения Индо-Австралийской литосферной плиты и зоной контакта.

При построении графика использованы данные об исторических землетрясениях [*Chlieh et al., 2007*]. Цвета кружков соответствуют значениям магнитуд на рис. 6.

Our analyses of seismotectonic deformations show that at all the depths, the most stable behaviour is demonstrated by the vertical extension component of STD. In the marginal areas at the western and eastern sides of the Sunda arc, the crustal layer (0–35 km) is subject to deformations which sign is opposite to that of deformations in the central part. The meridional component of STD is more uniform and characterized mainly by negative values.

In the 70–150 km layer beneath the epicentral area of the Sumatra earthquake, deformations change signs as compared to those in the studied segment of the Sunda arc.

For earthquakes that may occur in the crust in the contact zone of the plates, maximum magnitudes depend on the direction of pressure imposed by the actively subducting plate, which is an additional criterion for determining the limit magnitude for the study region.

The research is supported by RFBR 13-05-00054, 14-05-00688 and SB RAS Integration Project 76.

8. References

Cheng Zong-yi, Zhu Wen-yao, 2001. Crustal deformation of Asia-Pacific area determined from the GPS data of APRGP97–APRGP99. *Acta Seismologica Sinica* 14 (3), 280–292. http://dx.doi.org/10.1007/s11589-001-0006-6.

Chlieh M., Avouac J. P., Hjorleifsdottir V., Song T. R. A., Ji C., Sieh K., Sladen A., Hebert H., Prawirodirdjo L., Bock Y., Galetzka J., 2007. Coseismic slip and afterslip of the Great (Mw 9.15) Sumatra-Andaman Earthquake of 2004. *Bulletin of the Seismological Society of America* 97 (1A), S152–S173. http://dx.doi.org/10.1785/0120050631.

Dewey J.W., Choy G., Presgrave B., Sipkin S., Tarr A.C., Benz H., Earle P., Wald D., 2007. Seismicity associated with the Sumatra-Andaman Island earthquake of 26 December 2004. *Bulletin of the Seismological Society of America* 97 (1A), S25–S41. http://dx.doi.org/10.1785/0120050626.

Engdahl E.R., Villaseñor A., DeShon H.R, Thurber C.H., 2007. Teleseismic relocation and assessment of seismicity (1918–2005) in the region of the 2004 Mw 9.0 Sumatra-Andaman and 2005 Mw 8.6 Nias Island great earthquakes. *Bulletin of the Seismological Society of America* 97 (1A), S43–S61. http://dx.doi.org/10.1785/0120050614.

Hafkenscheid, Buiter S.J.H., Woltel M.J.R., Spakman W., Bijwaard H., 2001. Modelling the seismic velocity structure beneath Indonesia: comparison with tomography. *Tectonophysics* 333 (1–2), 35–46. http://dx.doi.org/10.1016/S0040-1951(00)00265-1.

Huchon P., Le Pichon X., 1984. Sunda Strait and Central Sumatra fault. *Geology* 12 (11), 668–672. http://dx.doi.org/10.1130/0091-7613(1984)12<668:SSACSF>2.0.CO;2.

Jaxybulatov K., Koulakov I., Ibs-von Seht M., Klinge K., Reichert C., Dahren B., Troll V.R., 2011. Evidence for high fluid/melt content beneath Krakatau volcano (Indonesia) from local earthquake tomography. *Journal of Volcanology and Geothermal Research* 206 (3–4), 96–105. http://dx.doi.org/10.1016/j.jvolgeores.2011.06.009.

Kostrov B.V., 1975. Mechanics of Tectonic Earthquake. Nauka, Moscow, 174 p. (in Russian) [*Костров Б.В.* Механика тектонического землетрясения. М.: Наука, 1975. 174 с.].

Koulakov I., 1998. Three-dimensional seismic structure of the upper mantle beneath the central part of the Eurasian continental. *Geophysical Journal International* 133 (2), 467–489. http://dx.doi.org/10.1046/j.1365-246X.1998.00480.x.

Koulakov I., Sobolev S.V., 2011. A tomographic image of Indian lithosphere break-off beneath the Pamir-Hindukush region. *Geophysical Journal International* 164 (2), 425–440. http://dx.doi.org/10.1111/j.1365-246X.2005.02841.x.

Koulakov I., Sobolev S.V., Weber M., Oreshin S., Wylegalla K., Hofstetter R., 2006. Teleseismic tomography reveals no signature of the Dead Sea Transform in the upper mantle structure. *Earth and Planetary Science Letter* 252 (1–2), 189–200. http://dx.doi.org/10.1016/j.epsl.2006.09.039.

Koulakov I., Tychkov S., Bushenkova N., Vasilevsky A., 2002. Structure and dynamics of the upper mantle beneath the Alpine-Himalayan orogenic belt, from teleseismic tomography. *Tectonophysics* 358 (1–4), 77–96. http://dx.doi.org/10.1016/S0040-1951(02)00418-3.

Kulakov I.Y., Tychkov S.A., Bushenkova N.A., Vasilevsky A.N., 2003. Three-dimensional velocity structure of upper mantle beneath the Alpine-Himalayan orogen. *Geologiya i Geofizika* (*Russian Geology and Geophysics*) 44 (6), 566–586.

Kundu B., Gahalaut V.K., 2011. Slab detachment of subducted Indo-Australian plate beneath Sunda arc, Indonesia. *Journal of Earth System Science* 120 (2), 193–204. http://dx.doi.org/10.1007/s12040-011-0056-7.

Radha Krishna M., Sanu T.D., 2002. Shallow seismicity, stress distribution and crustal deformation pattern in the Andaman-West Sunda arc and Andaman Sea, northeastern Indian Ocean. *Journal of Seismology* 6 (1), 25–41. http://dx.doi.org/10.1023/A:1014203306506.

Rebetskii Y.L., Marinin A.V., 2006. Stressed state of the Earth's crust in the western region of the Sunda subduction zone before the Sumatra-Andaman earthquake on December 26, 2004. *Doklady Earth Sciences* 407 (1), 321–325. http://dx.doi.org/10.1134/S1028334X06020383.

Riznichenko Yu.V., 1985. Problems of Seismology. Nauka, Moscow, 408 p. (in Russian) [*Ризниченко Ю.В.* Проблемы сейсмологии. М.: Наука, 1985. 408 с.]

Shevchenko V.I., Lukk A.A., Prilepin M.T., 2006. The Sumatra earthquake of December 26, 2004, as an event unrelated to the plate-tectonic process in the lithosphere. *Izvestiya, Physics of the Solid Earth* 42 (12), 1018–1037. http://dx.doi.org/10.1134/S1069351306120068.

The Global Centroid-Moment-Tensor (CMT) Project, 2015. Available from: http://www.globalcmt.org.

Vallee M., 2007. Rupture properties of the giant Sumatra earthquake imaged by empirical Green's function analysis. *Bulletin of the Seismological Society of America* 97 (1A), S103–S114. http://dx.doi.org/10.1785/0120050616.

Van der Hilst R.D., Widyantoro S., Engdahl E.R., 1997. Evidence for deep mantle circulation from global tomography. *Nature* 386 (6625), 578–584. http://dx.doi.org/10.1038/386578a0.

Кучай Ольга Анатольевна, канд. физ.-мат. наук, с.н.с.
Институт нефтегазовой геологии и геофизики им. А.А. Трофимука СО РАН
630090, Новосибирск, проспект академика Коптюга, 3, Россия
Тел. +7(383)3333792; ✉ e-mail: KuchayOA@ipgg.nsc.ru

Kuchay, Olga A., Candidate of Physics and Mathematics, Senior Researcher
Trofimuk Institute of Petroleum Geology and Geophysics, Siberian Branch of RAS
3 Acad. Koptyug prosp., Novosibirsk 630090, Russia
Tel. +7(383)3333792; ✉ e-mail: KuchayOA@ipgg.nsc.ru

Бушенкова Наталья Анатольевна, канд. геол.-мин. наук, с.н.с.
Институт нефтегазовой геологии и геофизики им. А.А. Трофимука СО РАН
630090, Новосибирск, проспект академика Коптюга, 3, Россия
Тел. +7(383)3309201; e-mail: BushenkovaNA@ipgg.sbras.ru
Новосибирский государственный университет
630090, Новосибирск, ул. Пирогова, 2, Россия

Bushenkova, Natalia A., Candidate of Geology and Mineralogy, Senior Researcher
Trofimuk Institute of Petroleum Geology and Geophysics, Siberian Branch of RAS
3 Acad. Koptyug prosp., Novosibirsk 630090, Russia
Tel. +7(383)3309201; e-mail: BushenkovaNA@ipgg.sbras.ru
Novosibirsk State University
2 Pirogov street, Novosibirsk 630090, Russia

Татаурова Антонина Андреевна, аспирант
Новосибирский государственный университет
630090, Новосибирск, ул. Пирогова, 2, Россия
e-mail: ant07@nm.ru

Tataurova, Antonina A., Post-Graduate Student
Novosibirsk State University
2 Pirogov street, Novosibirsk 630090, Russia
e-mail: ant07@nm.ru